DYNAMIC INFLOW AND GROUND EFFECT IN MULTIROTOR UAV ATTITUDE DYNAMICS

Fabio Riccardi fabio.riccardi@polimi.it

Marco Lovera marco.lovera@polimi.it

Department of Aerospace Science and Technology, Politecnico di Milano
Via La Masa 34, Milano, Italy

ABSTRACT: this paper deals with the problem of modelling the attitude dynamics of a quadrotor in ground effect. More precisely, dynamic ground effect on the quadrotor pitch attitude dynamics is modeled taking into account the dynamic inflow of the rotors and the simulation results are compared to the experimental ones obtained in previous studies.

1. INTRODUCTION

The flight control performance of multirotor UAVs is known to be subject to degradation when operating close to the ground. This issue is critical for autonomous missions, in which precise take-off, landing or hovering close to surfaces are involved. In spite of this, while ground effect has been studied extensively, both numerically and experimentally, for full-scale helicopters[1], the phenomenon has received limited attention as far as small-scale multirotors are concerned and only a few references are available at the moment.

More precisely, in previous studies of ground effect for multirotors[2,3,4] the main concern is to assess the mean value of thrust as a function of height from ground, *i.e.*, to carry out an experimental static characterization of ground effect and suggest, for different multirotor architectures, proper modifications to the classical Cheeseman & Bennet or Hayden formulas[1] to fit the data. While in[5] a frequency-domain analysis of a quadrotor roll attitude dynamics as a function of height from ground is proposed.

In view of these considerations, and in order to enhance the fidelity of ground effect models for an inhouse developed quadrotor[6] (MTOW of 1.5 kg, rotors radius of 0.15 m), and to improve the performance of its altitude/attitude control systems in ground proximity operations, two activities were previously carried out.

The first one[7], consisted in an experimental campaign aimed at a static characterization of ground effect (in terms of IGE/OGE thrust ratio) considering both the isolated rotor and the complete quadrotor. In the isolated rotor case, the obtained data qualitatively follow the trend of the classical formulations of ground effect from the literature. Regarding the complete quadrotor case, on the other hand, it seems that classical formulas valid for full-scale helicopters are not able to model correctly the phenomena for small multirotor vehicles. In particular the effect of the ground on the total thrust is extended up to almost 4 rotor radii of height, almost doubling the limit of about $h/R = 2.5$ found for the isolated rotor tests, and the discrepancy between the two cases reaches the maximum of about 5% T_{OGE} in the range $1 \leq h/R \leq 3$.

In the second work[8], the ground effect characterization for the considered quadrotor has been tackled in a dynamic perspective, carrying out an experimental model identification campaign. The quadrotor was placed on a test-bed constraining all DoFs except for pitch rotation (set-up representative of the actual pitch attitude dynamics in flight for near hovering conditions[9]) at different heights with respect to the ground. The pitch dynamics was then excited through a Pseudo Random Binary Sequence (PRBS), operating in closed-loop, *i.e.* with the pitch attitude controller active, in order to avoid excessive rotations during the experiments. A black-box method was applied to the gathered input/output datasets, in particular the Predictor-Based Subspace IDentification (PBSID) algorithm[10], obtaining second order LTI SISO models (from delta angular velocity of opposite rotors input $\delta\Omega$ to the vehicle pitch rate output q) for the pitch attitude dynamics in hovering at different heights from ground. It was observed that the dominant pole, representing the pitch dynamics, becomes slower when reducing the distance from ground. Therefore, it appears that besides affecting the rotors thrust (hence the vertical dynamics, as is well known in the rotorcraft literature and also verified in the previous study[7]), the distance from ground has an impact also on the hovering attitude dynamics for a quadrotor platform, as experienced in the flight practice.

Based on the above-described previous works, in this paper the results of a further investigation on the quadrotor attitude dynamics as a function of height in ground effect are presented, with specific reference

to the derivation of a first-principle model. More precisely, dynamic ground effect on the quadrotor pitch attitude dynamics is modeled taking into account the dynamic inflow of the rotors[11], hence the unsteady aerodynamics due to the wake-induced velocity of the rotors.

The paper is organized as follows. In Section 2 the considered quadrotor platform is first described. Subsequently, Section 3 describes the adopted inflow model and how it influences the quadrotor attitude dynamics in hover, while Section 4 presents the effect of ground proximity on the inflow dynamics. Finally in Section 5 the combined effect of the dynamic inflow and the ground on the attitude dynamics is considered and the obtained analytical models are compared with the identified ones varying the height from ground.

2. CONSIDERED QUADROTOR PLATFORM

The considered quadrotor is shown in Figure 1. The relevant parameters are reported in Table 1. The Flight Control Unit (FCU) uses as electronic boards the Rapid Robot Prototyping (R2P) modules[12]. R2P is an open source HW/SW framework providing components for the rapid development of robotic applications.

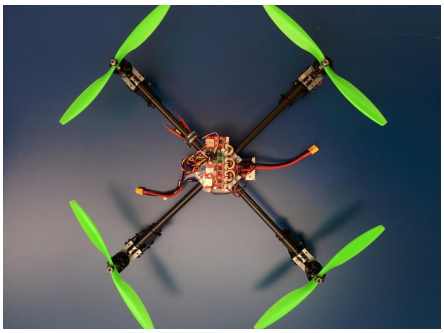

Figure 1: The quadrotor used in this study.

The isolated propeller performance data (thrust and power as a function of angular speed) are available from a previously conducted test campaign on a dedicated test bench and for the considerations that follow it is important to recall the resulting OGE hover trim parameters:

- single rotor thrust coefficient, $C_{T_{hov_{OGE}}} = 0.0122$;
- rotor angular velocity, $\Omega_{hov_{OGE}} = 380.9139\ rad/s$;
- thrust coefficient derivative respect to the angular velocity (from linearization around hovering), $(\partial C_T/\partial\Omega)_{hov_{OGE}} = 6.8840e-05$.

2.1 Identified model for OGE attitude dynamics

The reference identified model of the quadrotor pitch attitude dynamics in OGE hover was obtained in a previous test campaign carried out on a test bench[6], constraining all degrees of freedom except for pitch rotation. The obtained SISO transfer function from the input, delta angular velocity between the opposite couple of rotors $\delta\Omega$, to the output, pitch rate q, is

Parameter		Value
Frame Config.		X
Frame Model		HobbyKing Talon V2.0
Arm length	b	$0.275\ mm$
Take-off weight	m	$1.51\ kg$
Inertia roll/pitch	$I_{xx} = I_{yy}$	$0.035\ kg\ m^2$
Rotor radius	R	$0.1524\ m$
Average blade chord	$\bar{c}$	$0.02\ m$
Solidity	σ	0.083
Blade airfoil lift curve slope	C_{L_α}	$5.73\ rad^{-1}$
Motors		HP2814
KV		$710\ rpm/V$
ESC		RCTimer NFS 30 A
Battery		Turnigy nano-tech 4000 mAh

Table 1: Main parameters of the considered quadrotor

$$\frac{q(s)}{\delta\Omega(s)} = \frac{0.6951}{s + 2.056}. \tag{1}$$

Also the brushless motor dynamics was identified and the resulting transfer function from the input, motor throttle percentage $Th_{\%}$, and the output, delta angular velocity between the opposite couple of rotors $\delta\Omega$, is

$$\frac{\delta\Omega(s)}{Th_{\%}(s)} = \frac{1}{0.05s + 1}. \tag{2}$$

Hence the overall input-output relation is

$$\frac{q(s)}{Th_{\%}(s)} = \frac{0.6951}{0.05s^2 + 1.103s + 2.056}. \tag{3}$$

Finally, the static relation between throttle and motor rotational speed (in rad/s), determined experimentally, is

$$\Omega = \hat{m}Th_{\%} + \hat{q} = 6.031Th_{\%} + 80.49. \tag{4}$$

It is also useful to recall the first principle attitude dynamics model adopted in[6] to perform the grey-box identification of the model in equation (1), because it will be exploited in Section 5.2. Since on the single DoF test-bed the roll and yaw rotational and all translational DoFs are constrained, the differential equation governing the evolution of the pitch attitude is

$$I_{yy}\dot{q} = \frac{\partial M}{\partial q}\, q + \frac{\partial M}{\partial u}\, \delta\Omega \tag{5}$$

$$\dot{\theta} = q. \tag{6}$$

The model can be written in state space form as

$$\dot{x} = Ax + Bu \tag{7}$$

$$y = Cx + Du, \tag{8}$$

where the state vector is defined as $x = \begin{bmatrix} q & \theta \end{bmatrix}^T$, the control variable is $u = \delta\Omega$ and

$$A = \begin{bmatrix} \frac{1}{I_{yy}}\frac{\partial M}{\partial q} & 0 \\ 1 & 0 \end{bmatrix}, \quad B = \begin{bmatrix} \frac{1}{I_{yy}}\frac{\partial M}{\partial u} \\ 0 \end{bmatrix}, \tag{9}$$

$$C = \begin{bmatrix} 0 & 1 \end{bmatrix}, \quad D = \begin{bmatrix} 0 \end{bmatrix}. \tag{10}$$

The stability derivative of the pitching moment M with respect to q can be written as

$$\frac{\partial M}{\partial q} = -4\rho A(\Omega_{hov}R)^2 \frac{\partial C_T}{\partial q} d, \tag{11}$$

where ρ is the air density, $d = b/\sqrt{2}$ is the projection of the quadrotor arm length on the pitch body axis (considering the X configuration), A is the rotor area and

$$\frac{\partial C_T}{\partial q} = \frac{C_{L_\alpha}}{8}\frac{\sigma}{\Omega_{hov}R}. \tag{12}$$

Similarly, the pitching moment control derivative is given by

$$\frac{\partial M}{\partial u} = 4C_{T_{hov}}\rho A R^2 \sqrt{2} b \Omega_{hov}. \tag{13}$$

2.2 Ground effect model based on experimental campaign

In previous work[7] the experimental characterization of ground effect was carried out for both the isolated rotor and the complete quadrotor. The results are summarized in Figure 2. As can be seen from the figure, experimental data in the isolated rotor case qualitatively follow the trend of the classical formulations (Cheeseman & Bennet and Hayden) of ground effect from the rotorcraft literature. For the complete quadrotor, on the other hand, this is no longer true: hence it seems that the classical formulas valid for full-scale helicopters are not able to model correctly the ground effect for small multirotor vehicles. In particular the effect of the ground on the thrust is extended up to almost 4 rotor radii of height for the quadrotor case, doubling the classical limit of about $h/R = 2$ found for the isolated rotor tests. This discrepancy between complete quadrotor and isolated rotor results is likely due to the variation of the airframe download in proximity of the ground and to the interferences between the four rotor wakes.

3. INCLUDING DYNAMIC INFLOW IN THE ATTITUDE DYNAMICS

In order to introduce the effect of ground proximity on the quadrotor pitch attitude dynamics, the rotors

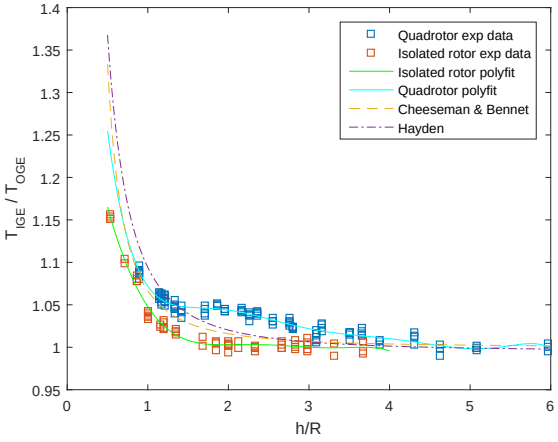

Figure 2: Rotor thrust ratio IGE/OGE at constant power as a function of non-dimensional height from ground h/R: comparison between isolated rotor, complete quadrotor experimental data and classical formulations.

dynamic inflow, hence the rotors unsteady aerodynamics due to the rotors wake-induced velocity, was added to the model[11], starting from the identified pitch attitude dynamics for OGE hover.

3.1 Adopted inflow model

The first order inflow model proposed by Pitt and Peters[13] was adopted. In particular, of the original three inflow states only the axial (uniform) perturbation contribution $\delta\lambda_u$ was retained: in fact the pitch attitude motion implies an axial flow regime on the rotors. Hence the considered scalar equation of the inflow dynamics is

$$L_u M_u \delta\dot{\lambda}_u + \delta\lambda_u = L_u \delta\hat{C}_T \tag{14}$$

where $L_u = \frac{1}{4\lambda_{i_{hov}}}$ and $M_u = \frac{8}{3\pi\Omega_{hov}}$. Recalling that the induced inflow ratio is given by

$$\lambda_{i_{hov}} = \sqrt{C_{T_{hov}}/2},$$

for the non-perturbed trimmed configuration in OGE hover the resulting time constant of the inflow dynamics for the considered small rotor is

$$\tau_{\lambda_u} = L_u M_u = 0.0069\ s.$$

Note that a typical value for a manned helicopter rotor[1] is in the order of $0.1\ s$. The Bode plots of the inflow dynamics (from the input $\delta\hat{C}_T$ to the output $\delta\lambda_u$) are shown in Figure 3; the dynamics is characterized by a single real pole at $1/\tau_{\lambda_u} = 144.03\ rad/s$).

The thrust coefficient perturbation, including the effect of hub vertical motion $\dot{z}_{hub}$ due to the pitch angular rate q, is given by

$$\delta\hat{C}_T = \delta C_T - C_{T_{hov}}\frac{\dot{z}_{hub}}{v_{i_{hov}}} = \frac{\partial C_T}{\partial\lambda_u}\delta\lambda_u - C_{T_{hov}}\frac{qd}{v_{i_{hov}}}, \tag{15}$$

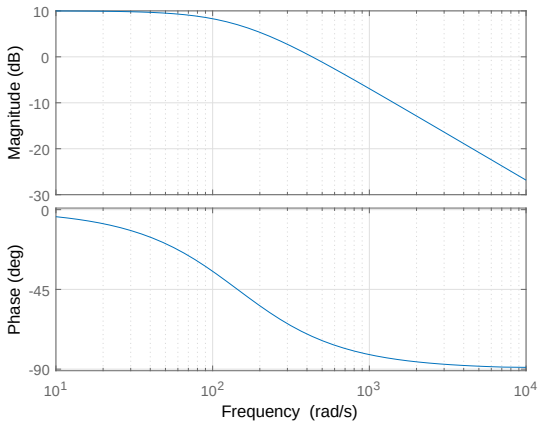

Figure 3: Bode plot of the frequency response function of the inflow dynamics for the OGE hover trim (from $\delta\hat{C}_T$ to $\delta\lambda_u$).

where the rotor induced velocity in hover is

$$v_{i_{hov}} = \lambda_{i_{hov}} \Omega_{hov} R,$$

and

$$\frac{\partial C_T}{\partial \lambda_u} = \frac{\sigma C_{L_\alpha}}{4}.$$

3.2 Adopted modeling scheme

The input of the inflow dynamic model is the thrust coefficient perturbation $\delta\hat{C}_T$, while the output is the uniform inflow perturbation $\delta\lambda_u$, hence a closed-loop system[14] with the previously identified model in OGE hover of the pitch attitude dynamics (including the motors) was defined, as described hereafter and shown in the block diagram of Figure 4.

The $\delta\Omega$ command input for the attitude dynamics model implies, through the derivative $\partial C_T/\partial\Omega$ (linearization of rotor C_T vs. Ω curve around the OGE hover condition), a δC_T which goes in input to the dynamic inflow, together with the term defining the δC_T contribution due to the axial velocity of the rotor hub, obtained multiplying by the projection of the quadrotor arm length on the pitch body axis d, the pitch angular velocity q (output of the attitude dynamics model). The loop closure is imposed considering that the inflow dynamic output $\delta\lambda_u$, through the derivative $\frac{\partial C_T}{\partial \lambda_u}$, gives a δC_T which acts as input to the inflow dynamics itself and also corresponds to a $\delta\Omega$ input to the attitude dynamics.

3.3 Results

The effects of including dynamic inflow in the pitch attitude dynamics (OGE hover trim) are shown in Figures 5, 6 and 7, obtained from a Matlab/Simulink model implementing the block diagram in Figure 4. With respect to the only identified attitude dynamics, characterized by two real poles (at $2.06\ rad/s$ the pitch dynamics, at $20\ rad/s$ the motor dynamics), closing the loop on the inflow dynamics results in three real poles (at $2.36\ rad/s$, $19.65\ rad/s$ and $133.5\ rad/s$) and one real zero (at $140.2\ rad/s$). Observing the step response, including the dynamic inflow implies a slightly slower and more damped pitch attitude response.

4. EFFECT OF THE GROUND ON THE INFLOW DYNAMICS

The effect of the ground on the inflow dynamics was introduced adding a further inflow perturbation in input[15], due to the changes in the rotor dimensionless height above ground $\bar{z} = h/R$, through the derivative $\partial\lambda_u/\partial\bar{z}$. Hence the new differential equation for the inflow perturbation is:

$$L_u M_u \delta\dot{\lambda}_u + \delta\lambda_u = L_u \delta\hat{C}_T - \frac{\partial\lambda_u}{\partial\bar{z}}\delta\bar{z}. \tag{16}$$

The derivative $\partial\lambda_u/\partial\bar{z}$ can be easily computed from the adopted ground effect model formula, in fact

$$\lambda_u = \lambda_{OGE}\frac{T_{OGE}}{T_{IGE}}$$

where $\lambda_{OGE} = \lambda_{i_{hov}}$. Figure 8 shows the uniform inflow λ_u as a function of the non-dimensional height from ground for the two classical formulations of ground effect, Cheeseman & Bennet and Hayden, compared with the models obtained by polynomial fitting of the experimental results on the quadrotor and its isolated rotor. Finally, Figure 9 shows the derivative $\partial\lambda_u/\partial\bar{z}$ as a function of height from ground.

In Figures 10 and 11 are shown respectively the Bode plots and the step response of the inflow dynamics described in equation (16), in particular from the added input $\delta\bar{z}$ to the output $\delta\lambda_u$ (inflow perturbation), at different non-dimensional height from ground, considering the ground effect model based on interpolation of experimental data gather for the complete quadrotor case.

5. ATTITUDE DYNAMICS CONSIDERING THE EFFECT OF BOTH DYNAMIC INFLOW AND GROUND

The effect of ground proximity on the quadrotor pitch (or roll) dynamics can be explained analyzing the derivative $\partial\lambda_u/\partial\bar{z}$: since it is a function of $\bar{z}$ and is greater than zero, when in ground effect a reduction in the rotor height above ground produces a decrease in the induced velocity, hence a rotor thrust increase that acts as a spring against the height variation, with increasing stiffness as the ground approaches. Considering the side-by-side rotors configuration of the quadrotor, the antisymmetric height change of opposite rotors associated with pitch (or roll) implies an alteration of the pitch (or roll) attitude dynamics as a

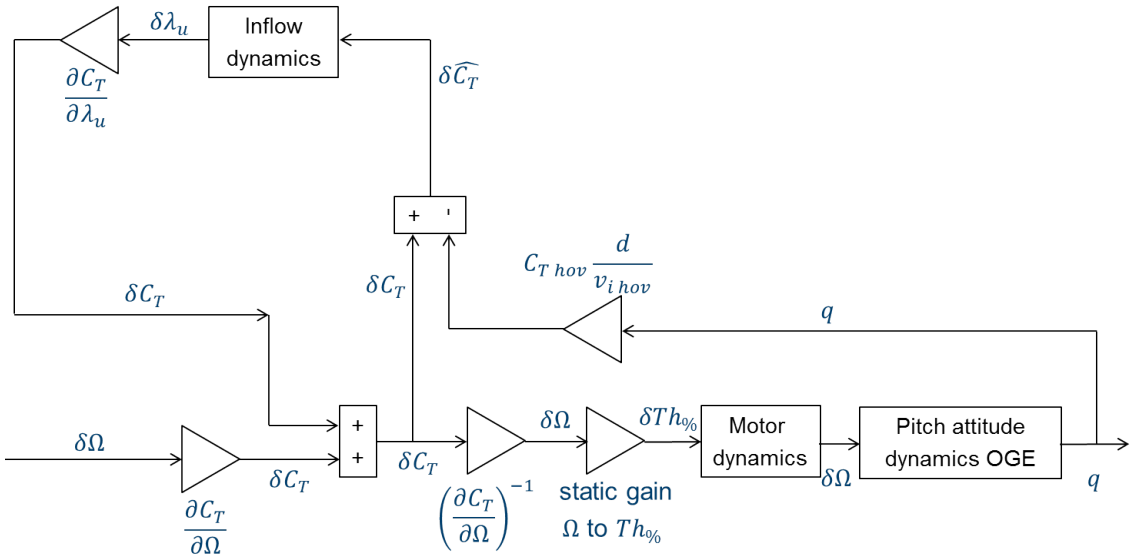

Figure 4: Block diagram of the closed-loop system between the rotor inflow dynamics and the pitch attitude dynamics.

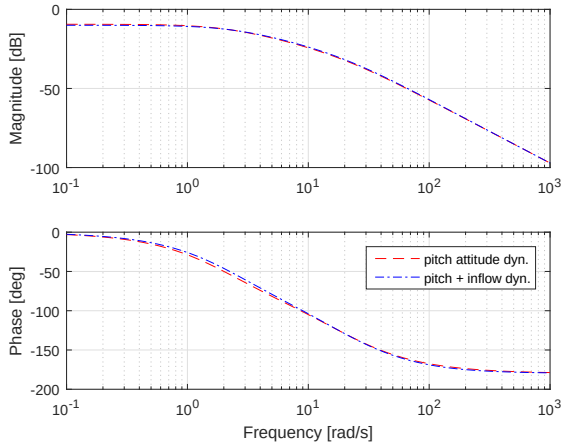

Figure 5: Bode plots of the frequency response function of the pitch attitude dynamics for the OGE hover trim with and without inflow dynamics.

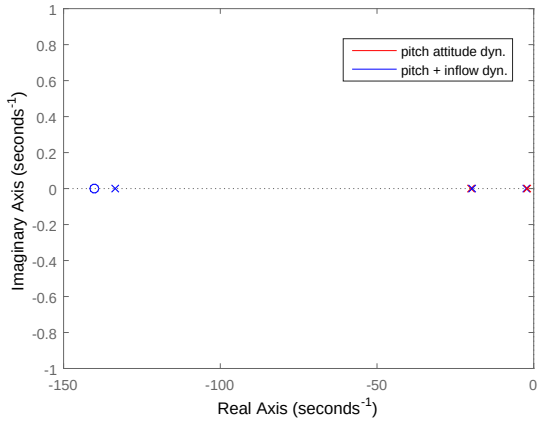

Figure 7: Pole-zero map of the pitch attitude dynamics for the OGE hover trim with and without inflow dynamics.

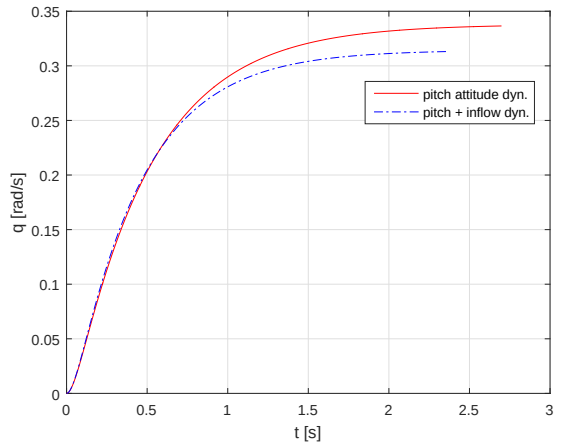

Figure 6: Step response of the pitch attitude dynamics for the OGE hover trim with and without inflow dynamics.

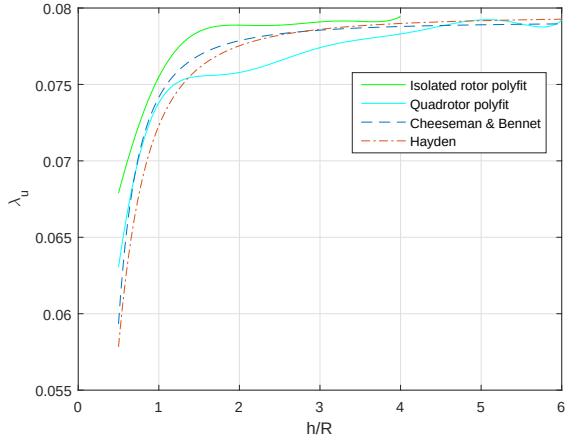

Figure 8: Uniform inflow λ_u as a function of the non-dimensional height from ground $\bar{z} = h/R$ for different ground effect models.

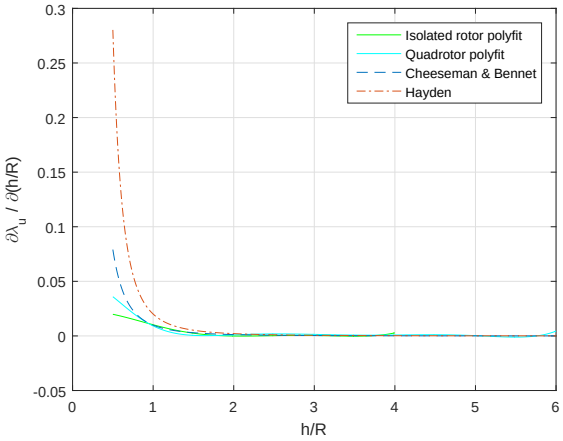

Figure 9: Derivative $\partial\lambda_u/\partial\bar{z}$ as a function of the non-dimensional height from ground $\bar{z} = h/R$ for different ground effect models.

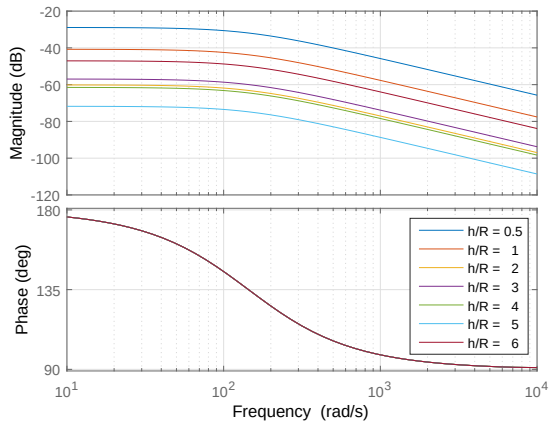

Figure 10: Bode plots of the frequency response function of the inflow dynamics for the OGE hover trim including the effect of the ground (from $\delta\bar{z}$ to $\delta\lambda_u$). Adopted ground effect model: polyfit on quadrotor experimental data.

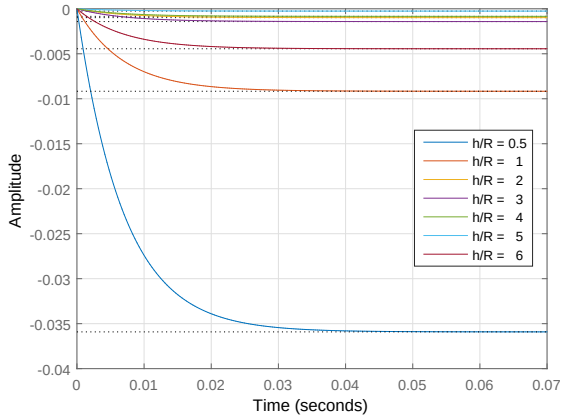

Figure 11: Step response of the inflow dynamics for the OGE hover trim including the effect of the ground (from $\delta\bar{z}$ to $\delta\lambda_u$). Adopted ground effect model: polyfit on quadrotor experimental data.

function of height in ground effect, as well known from flight experiences and confirmed by the identification results.

5.1 Adopted modeling scheme

Figure 12 shows the modeling scheme developed to evaluate the effect of the ground, through the inflow dynamics, on the quadrotor pitch attitude dynamics. Comparing it with the block diagram of Figure 4, where the effect of the inflow dynamics (see equation (14)) on the vehicle pitch rotation was considered without taking into account the height from ground (only thrust coefficient perturbation, equation (15)), it is possible to recognize the added rotors height perturbation $\delta\bar{z}$ (around the hovering condition at a given height $\bar{z}$) to the inflow dynamics (in accordance with equation (16)), simply computed multiplying the quadrotor arms length by the sine of pitch angle (by integration of the pitch rate) and dividing by rotor radius.

5.2 Correction of identified attitude dynamics model in OGE for the hover IGE

When hover is performed in ground effect, the quadrotor trim parameters, namely the rotors angular velocity and hence the thrust coefficient (and the induced inflow ratio), change with respect to the OGE condition, affecting the inflow dynamics parameters L_u and M_u (see equation (14)) and the gain equal to the thrust coefficient derivative respect to the angular velocity used in the closed-loop modeling scheme in Figure 12. In Figures 13 and 14 the above trim values are shown as functions of the non-dimensional height from ground, computed using the ground effect model based on interpolation of experimental data gather for the complete quadrotor case.

Moreover the variation of the hover trim parameters during IGE operation affects also the attitude pitch dynamics model, as can be argued observing the first-principle (theoretical) formulation of the LTI system described in Section 2.1: the stability derivative $\partial M/\partial q$ (equation (11)) and the control derivative $\partial M/\partial u$ (equation (13)) depend on the rotors angular velocity and the thrust coefficient in hover, hence in Figure 15 are shown $\partial M/\partial q$ and $\partial M/\partial u$ as functions of the height from ground.

As a consequence of the variation of the pitch attitude model derivatives with respect to the height from ground, computed considering the IGE hover trim value of rotors angular velocity and thrust coefficient, it is possible to determine the theoretical variation of the pitch attitude model, in terms of the SISO transfer function gain and poles, with respect to the OGE reference model, as reported in Figure 16. The same variation computed on the theoretical transfer function was applied to the experimentally identified transfer

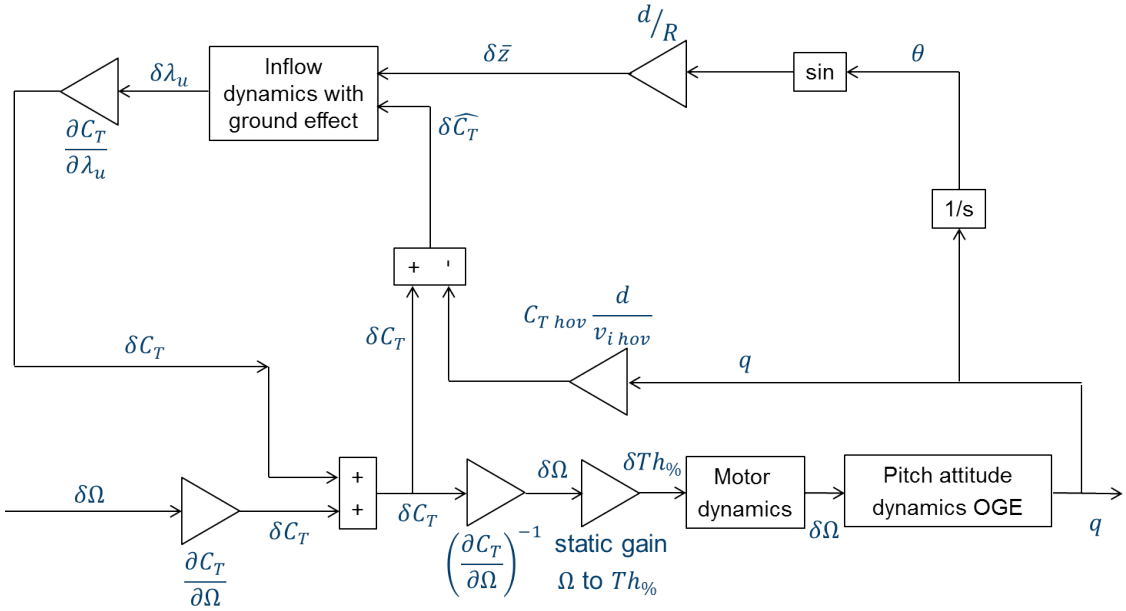

Figure 12: Block diagram of the closed-loop system between the rotor inflow dynamics and the pitch attitude dynamics, including the effect of the ground

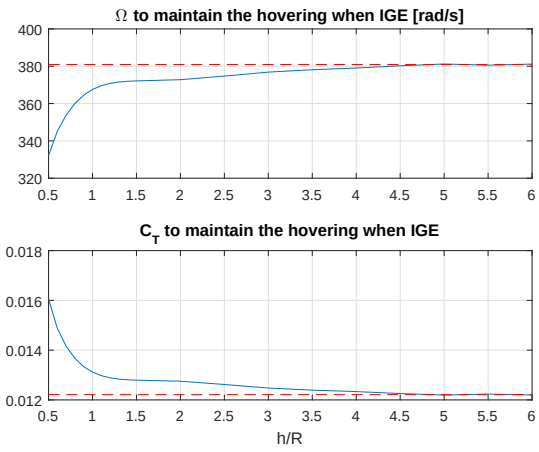

Figure 13: Rotor angular velocity Ω and thrust coefficient C_T required to maintain IGE hover, hence the same thrust OGE, at various heights from ground. The red dashed lines represent the OGE reference values.

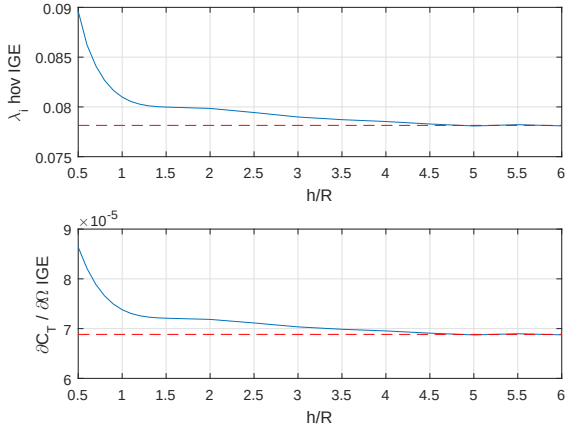

Figure 14: Rotor induced inflow ratio $\lambda_{i_{hov}}$ in IGE hover and thrust coefficient derivative respect to the angular velocity $\partial C_T/\partial\Omega$ (from linearization around hovering IGE), at various heights from ground. The red dashed lines represent the OGE reference values.

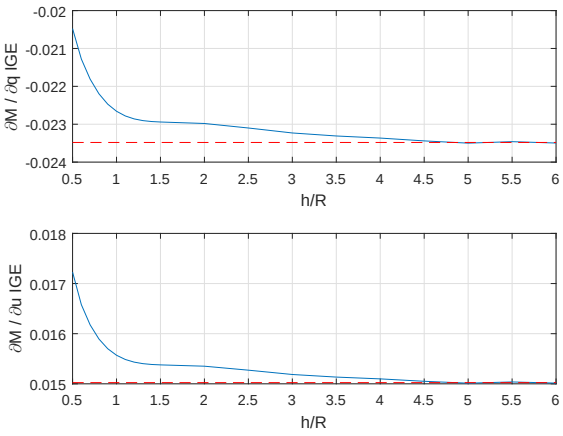

Figure 15: Stability and control derivatives of the LTI pitch attitude dynamics model with respect to the height from ground. The red dashed lines represent the OGE reference values.

function of the pitch attitude dynamics in OGE hover (see equation (1)), in order to retrieve the effects of the trim parameters variation during IGE hover. Finally the Bode plots and the step response of the identified pitch attitude dynamics for IGE hover (considering only the trim parameters variation in ground effect), as a function of the height from ground, are reported respectively in Figures 17 and 18.

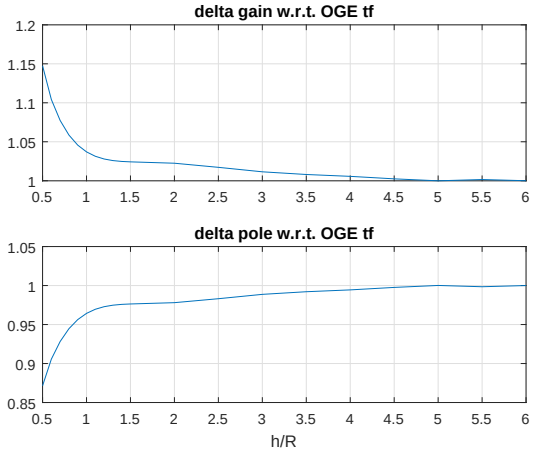

Figure 16: Pitch attitude theoretical model variation, in terms of the SISO transfer function gain and real pole values, respect to the OGE reference model.

5.3 Results

In this section the results obtained by linearization of the Matlab/Simulink model implementing the block diagram of Figure 12 are reported: a fourth order LTI model from delta angular velocity of opposite rotors $\delta\Omega$ to the vehicle pitch rate q is obtained, representing the pitch attitude dynamics taking into account the effect of the ground, through the inflow dynamics. The identified pitch dynamics in OGE hover was properly modified in order to take into account the trim param-

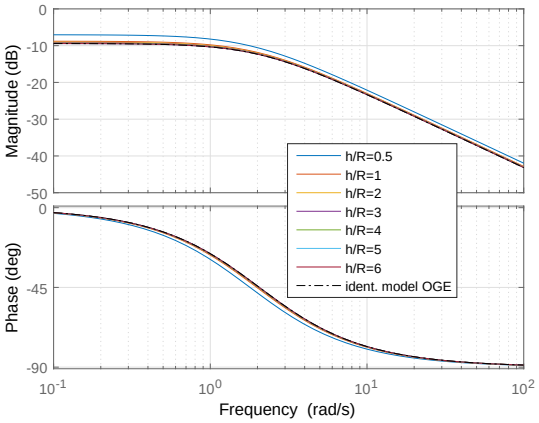

Figure 17: Bode plots of the identified pitch attitude dynamics for IGE hover (considering only the trim parameters variation in ground effect).

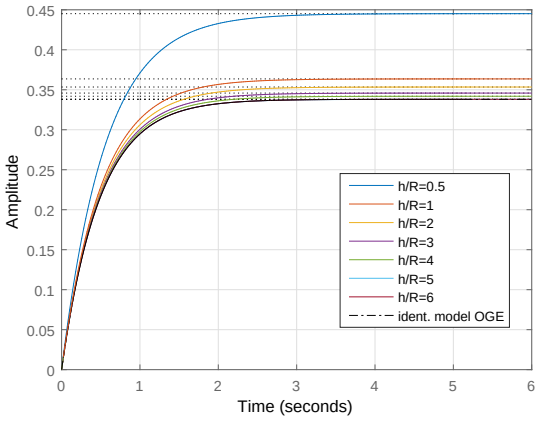

Figure 18: Step response of the identified pitch attitude dynamics for IGE hover (considering only the trim parameters variation in ground effect).

eters changes for IGE hover as a function of height from ground, as described in Section 5.2. In Figure 19 the Bode plots and the step response of the final pitch attitude model are reported, taking into account inflow dynamics and ground effect, at different values of height from ground: as reference the pitch model (comprehensive of motor dynamics but without ground effect) without (second order) and with (third order) inflow is also shown. On the step response one can recognize the effect of the ground proximity on the attitude dynamics, as equivalent to a spring connected to the ground under each rotor, with a stiffness which decreases for increasing height (into the IGE range).

The final fourth order LTI model is characterized by two zeros and four poles. The zeros are both real (see Figure 20), independently on the height from ground, at $140.3\ rad/s$ and $0\ rad/s$: as a reference the single real zero of the pitch dynamics with the inflow was at $140.2\ rad/s$.

Concerning the poles (see Figure 21), the final model has one complex conjugate pair and two real poles in the range $0.5 \leq h/R \leq 1$, while four pure real poles when $h/R > 1$. The real part of the poles 1, 2 and 3 tend to the value of the corresponding poles of the third order pitch dynamics (including the inflow), respectively at $2.36\ rad/s$, $19.65\ rad/s$ and $133.5\ rad/s$. Pole 1 represents the pitch attitude dynamics, which was at $2.06\ rad/s$ from the identified model in OGE hover, while pole 2 can be associated with the motor dynamics, at $20\ rad/s$ from the identified OGE model.

5.4 Comparison with identified attitude dynamics model varying the height from ground

Finally, in Figure 22 a comparison between the above-described analytical LTI model for the quadrotor pitch attitude dynamics in IGE hover (from delta angular velocity of opposite rotors $\delta\Omega$ to the vehicle pitch rate q) and the results from the previously conducted experimental identification campaign (see[8], briefly resumed in Section 1) is presented. In particular the behavior, as a function of the height from ground, of the identified second order model poles (the lower frequency one associated to the attitude dynamics and the higher frequency one to the motor dynamics), and the correspondent poles of the analytical model is illustrated. The developed analytical model shows the same trend of both poles, as a function of vehicle height from ground, resulted from identification: the dominant pole representing the pitch dynamics, becomes slower when reducing the distance from ground, while the second pole, corresponding to the motors dynamics, becomes faster when the height decreases. The variation of the dominant pole frequency with respect to height predicted by the analytical model matches the identification results. On

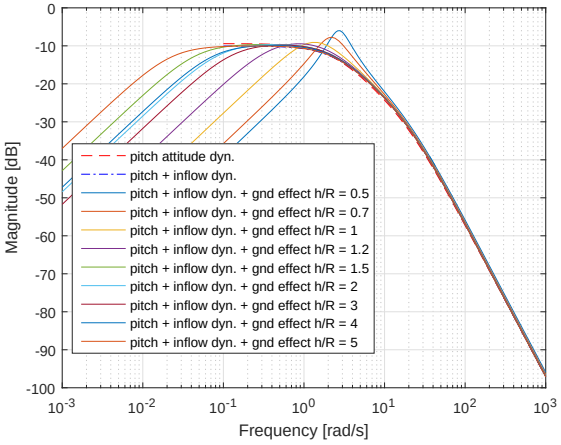

(a) Bode magnitude.

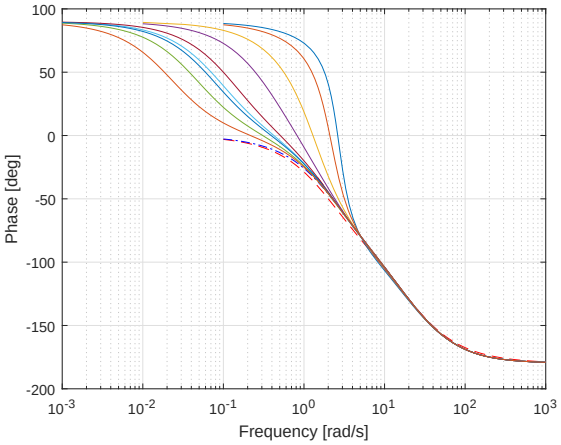

(b) Bode phase.

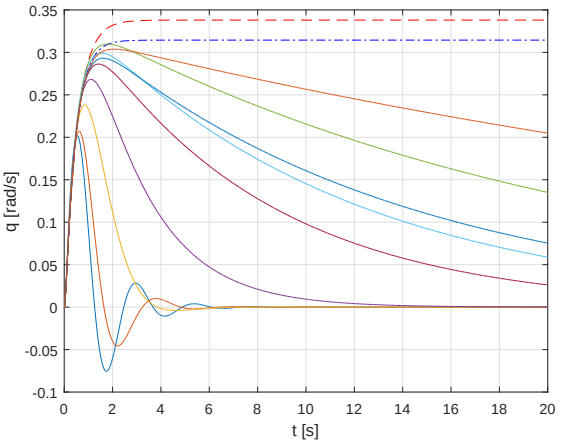

(c) Step response.

Figure 19: Bode plots and step response of the hovering pitch attitude dynamics taking into account the effect of the ground, through the inflow dynamics, at different non-dimensional height from ground. As reference the pitch dynamics (with and without inflow) is also depicted.

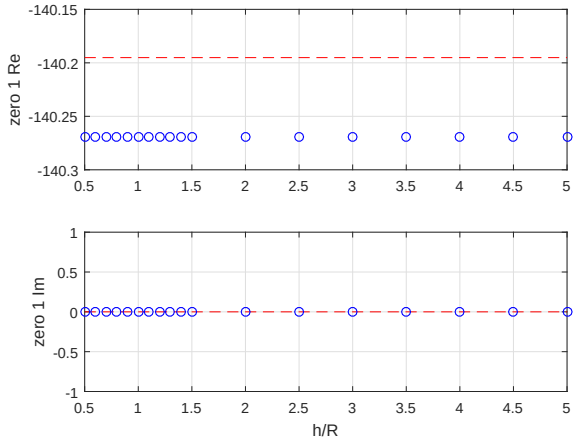

(a)

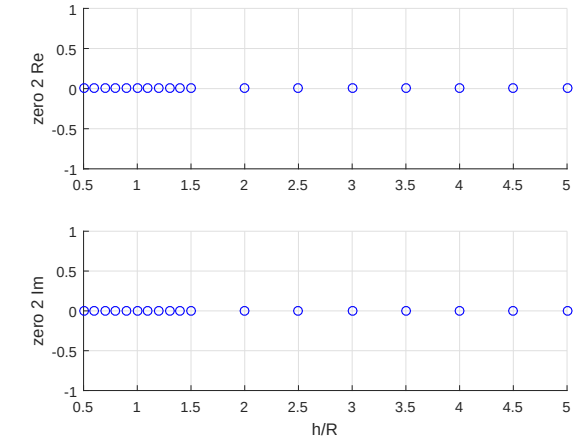

(b)

Figure 20: Zeros of the hovering pitch attitude dynamics taking into account the effect of the ground, through the inflow dynamics, at different non-dimensional height from ground. As reference the single zero of the pitch dynamics including the inflow is also shown (red dashed line).

the contrary, the analytical approach predicts a much smaller variation with height of the pole associated with motor dynamics with respect to the identification results: it must be taken into account that this frequency range was weakly excited during the experiments hence the uncertainty of identified model is wider.

6. CONCLUDING REMARKS AND FURTHER ACTIVITIES

In this paper the problem of modelling the attitude dynamics of a quadrotor in ground effect has been considered. From the modelling point of view, dynamic ground effect on the quadrotor pitch attitude dynamics has been taken into account by including the (Pitt-Peters) dynamic inflow of the rotors in the overall model. The simulation results are representative of the observed behaviour in IGE quadrotor flight and match reasonably well compared to the experimental results obtained in previous studies.

Future work will aim at exploiting the array of LTI models in state-space form obtained linearizing the closed-loop system of the attitude+inflow dynamics for different height from ground to implement gain-scheduled attitude controllers for enhanced performance during take-off, landing or close-to-ground operations.

REFERENCES

[1] G. J. Leishman. *Principles of helicopter aerodynamics*. Cambridge University Press, 2006.

[2] C. Powers, D. Mellinger, A. Kushleyev, B. Kothmann, and V. Kumar. Influence of aerodynamics and proximity effects in quadrotor flight. In *Experimental Robotics*, pages 289–302. Springer, 2013.

[3] L. Danjun, Z. Yan, S. Zongying, and L. Geng. Autonomous landing of quadrotor based on ground effect modelling. In *34th Chinese Control Conference (CCC)*, pages 5647–5652. IEEE, 2015.

[4] I. Sharf, M. Nahon, A. Harmat, W. Khan, M. Michini, N. Speal, M. Trentini, T. Tsadok, and T. Wang. Ground effect experiments and model validation with Draganflyer X8 rotorcraft. In *2014 International Conference on Unmanned Aircraft Systems (ICUAS)*, pages 1158–1166. IEEE, 2014.

[5] S. Aich, C. Ahuja, T. Gupta, and P. Arulmozhivarman. Analysis of ground effect on multi-rotors. In *2014 International Conference on Electronics, Communication and Computational Engineering (ICECCE)*, pages 236–241. IEEE, 2014.

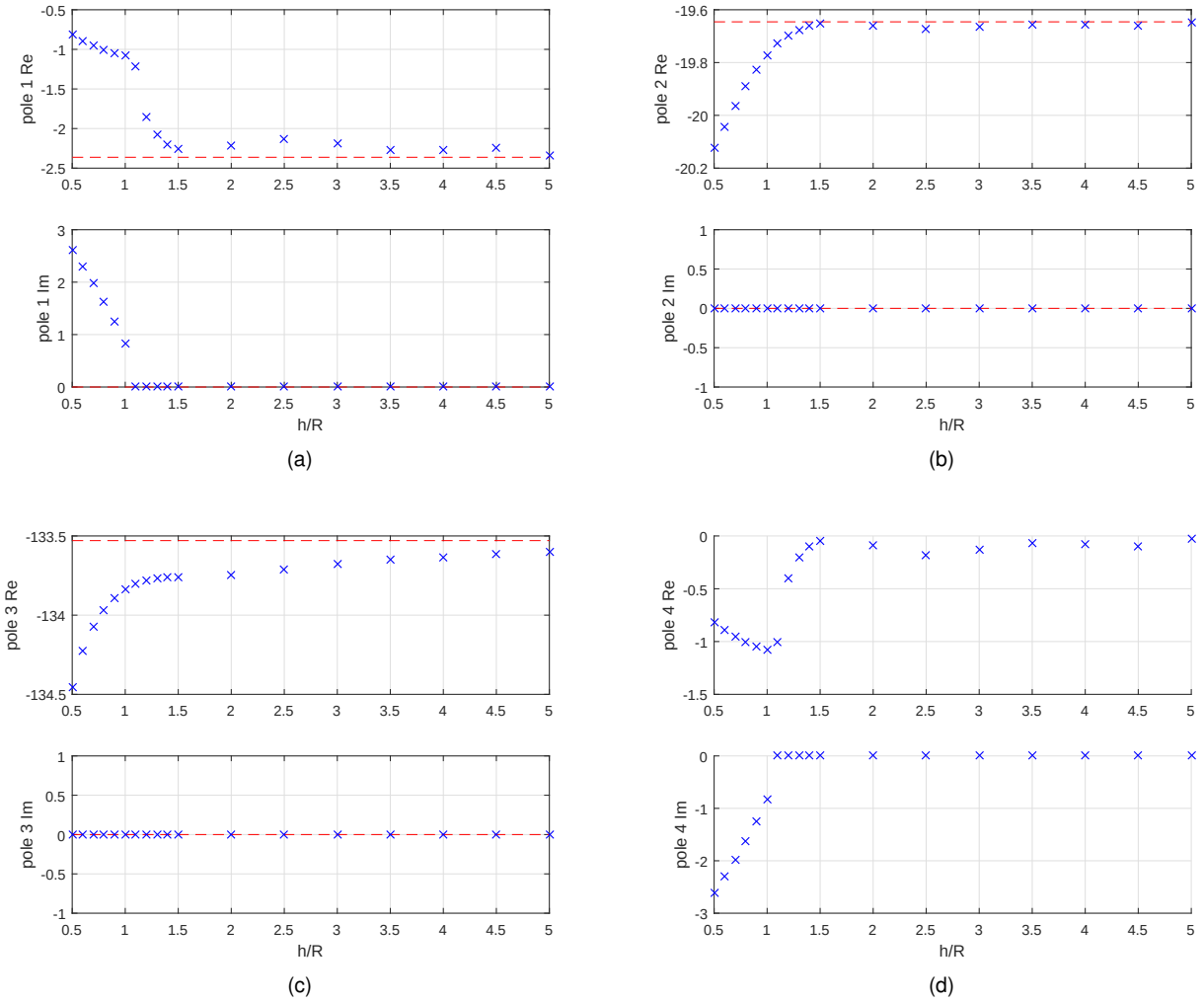

Figure 21: Poles of the hovering pitch attitude dynamics taking into account the effect of the ground, through the inflow dynamics, at different non-dimensional height from ground. As reference the three poles of the pitch dynamics including the inflow are also shown (red dashed line).

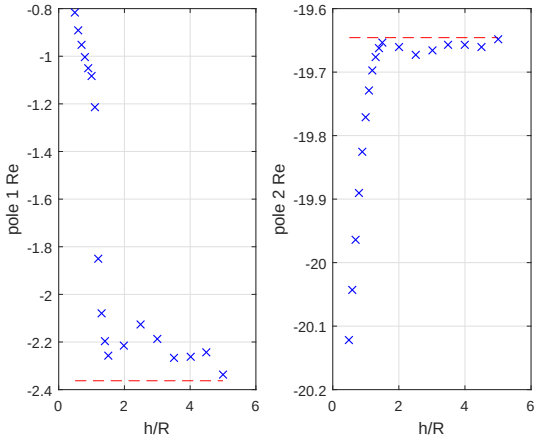

(a) Analytical model.

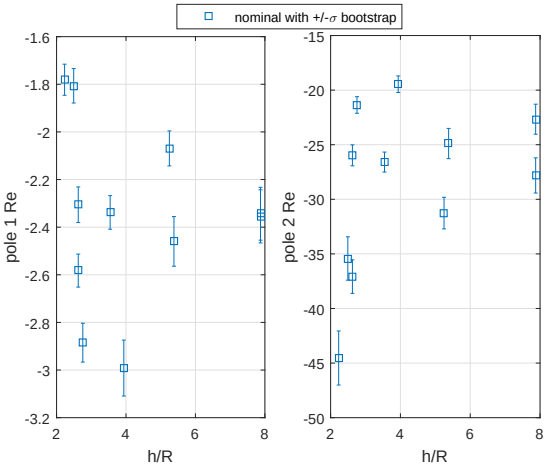

(b) Experimentally identified model. The error bar around each value represents the $\pm\sigma$ model uncertainty bound, determined via bootstrap technique.

Figure 22: Poles of the quadrotor pitch attitude dynamics in hovering IGE as a function of the dimensionless height from ground, from experimental identification and analytical model: the lower frequency one (pole 1) associated to the attitude dynamics and the higher frequency one (pole 2) to the motor dynamics.

[6] M. Giurato. Design, integration and control of a multirotor UAV platform. Master's thesis, Politecnico di Milano, Italy, 2015.

[7] D. Del Cont, M. Giurato, F. Riccardi, and M. Lovera. Ground effect analysis for a quadrotor platform. In *4th CEAS Specialist Conference on Guidance, Navigation & Control, Warsaw, Poland*, 2017.

[8] D. Del Cont, F. Riccardi, M. Giurato, and M. Lovera. A dynamic analysis of ground effect for a quadrotor platform. In *20th IFAC World Congress, Toulouse, France*, 2017.

[9] F. Riccardi and M. Lovera. Robust attitude control for a variable-pitch quadrotor. In *IEEE Multi-Conference on Systems and Control, Antibes, France*. IEEE, 2014.

[10] Chiuso, A. The role of autoregressive modeling in predictor-based subspace identification. *Automatica*, 43(3):1034–1048, 2007.

[11] R. Niemiec and F. Gandhi. Effects of inflow model on simulated aeromechanics of a quadrotor helicopter. In *AHS 72nd Annual Forum, West Palm Beach, Florida*, 2016.

[12] A. Bonarini, M. Matteucci, M. Migliavacca, and D. Rizzi. R2P: An open source hardware and software modular approach to robot prototyping. *Robotics and Autonomous Systems*, 62(7):1073–1084, 2014.

[13] D. M. Pitt and D. A. Peters. Theoretical prediction of dynamic-inflow derivatives. *Vertica*, 5(1):21–34, 1981.

[14] G. H. Gaonkar and D. A. Peters. Review of dynamic inflow modeling for rotorcraft flight dynamics. In *AIAA 27th SDM Conference, San Antonio, Texas, AIAA-86-0845-CP*, 1986.

[15] W. Johnson. *CAMRAD/JA A comprehensive analytical model of rotorcraft aerodynamics and dynamics - Theory Manual Vol.1*. Johnson Aeronautics, 1988.